DOI 10.1007/s11595-014-1010-8

Preparation of V-doped TiO_2 Photocatalysts by the Solution Combustion Method and Their Visible Light Photocatalysis Activities

MA Xiao, XUE Lihong*, YIN Shengming, YANG Miao, YAN Youwei

(State Key Laboratory of Materials Processing and Die and Mould Technology, Huazhong University of Science and Technology, Wuhan 430074, China)

Abstract: A series of nanocrystalline V-doped (0.0-3.0 at.%) TiO_2 catalysts have been successfully prepared by the one-step solution combustion method using urea as a fuel. The obtained powders were characterized by XRD, SEM, Raman, XPS and UV-Vis DRS. The effects of V doping concentration on the phase structure and photocatalytic properties were investigated. XRD, Raman, and XPS show that V doping diffuses into TiO_2 crystal lattice mainly in the form of V^{5+} and causes a phase transition from anatase to rutile. V doping can widen the light absorption range of TiO_2, with the absorption threshold wavelength shifting from 425 to 625 nm. The photocatalytic activity of V-doped TiO_2 powders were evaluated by the photocatalytic degradation of methyl orange (MO) under visible light irradiation. It is found that V doping enhances the photocatalytic activity under visible light irradiation and the optimal degradation rate of MO is about 95.8% with 1.0 at% V-doped TiO_2.

Key words: solution combustion; titanium dioxide; V doping; photocatalyst

1 Introduction

Titanium oxide (TiO_2), one of the most popular photocatalysts, is widely used in antimicrobial, deodorization, air and water purification owing to its photostability, non-toxicity, low cost, redox efficiency, and availability[1-4]. However, more widespread applications of TiO_2 as photocatalysts are limited because of its relatively wide band gap (3.2 eV) and low photo-quantum yield value. To overcome these two shortcomings, many attempts have been made for practical applications[5, 6].

It is generally accepted that metal ion doping can bring about defects in the lattice or improve the crystallinity of the catalysts, which can increase the photocatalytic efficiency[7,8]. A number of different transition metal ions including Cu^{2+}, Mn^{2+}, V^{5+}, Ce^{3+} and Sn^{4+} have been attempted to dope in TiO_2 to create a batho-chromic shift of the band gap energy. Among those dopants, V ion is one of the most frequent research topics, because V ionic radius is almost the same as Ti ion's and thus can be easily doped in TiO_2 to increase the carrier lifetime and extend the absorption range[9-17]. Anpo[12] prepared V-doped TiO_2 photocatalysts through ion implantation. This physically doped catalysts are much more photoefficient than those prepared using traditional chemical techniques. Zhou[13] synthesized V-doped TiO_2 nanoparticles by sol-gel method using $Ti(OBu)_4$ as a precursor. The absorption threshold wavelength is red shifted from 380 to about 650 nm.

The photocatalytic activity of photocatalysts can be affected by the synthesis methods and experimental conditions[14]. Many wet chemical methods, like sol-gel technique[13,15], ion-implantation methods[12,16] and liquid phase deposition[17] have been applied for obtaining V-doped TiO_2 catalysts. However, these techniques require long-period post-treatment or costly reagents. Solution combustion synthesis is one of the simplest

(Received: Oct. 25, 2013; Accepted: June 15, 2014)

MA Xiao(马晓): Candidate for Ph D; E-mail: 383201089@qq.com

*Corresponding author: XUE Lihong (薛丽红): Assoc.Prof.; Ph D; E-mail: xuelh@mail.hust.edu.cn

Funded by the National Natural Science Foundation of China (Nos. 51002054, 51272079) and the Fundamental Research Funds for the Central Universities, HUST (No. 2011TS014)

and the most cost-effective synthesis routes for the preparation of nanocrystalline powders because in combustion synthesis, the thermal energy required for the reaction to occur is provided by the reaction itself, instead of the external source. We have successfully synthesized TiO_2 powders with different anatase/rutile ratios by this method. No further calcining process is required to promote phase formation. In this paper, a series of V-doped (0.0-3.0 at%) TiO_2 catalysts were synthesized by the solution combustion method in a single step. The effects of V doping concentration on the phase structure and photocatalytic properties were investigated.

2 Experimental

2.1 Catalyst preparation

V-doped TiO_2 powders were prepared by the solution combustion method using urea ($CO(NH_2)_2$, AR) as a fuel. Tetrabutyl titanate ($Ti(C_4H_9O)_4$, 98%) and ammonium metavanadate (NH_4VO_3, AR) were used as the starting materials. Firstly, $Ti(C_4H_9O)_4$ was added into distilled water to get a white precipitate. The precipitate was washed with distilled water and then dissolved in HNO_3 to get a clear solution. Secondly, appropriate amounts of NH_4VO_3 and $CO(NH_2)_2$ were added into the clear solution and stirred for 10 min to form a homogeneous solution. Thirdly, the mixture solution was introduced into a muffle furnace preheated to 600 ℃. Within a few minutes, the solution boiled and was ignited to produce a self-propagating flame. Finally, the powder was obtained. To study the effects of V doping on the phase and photocatalytic properties of TiO_2 powders, the molar ratios of V/Ti were adjusted to 0.1%, 0.3%, 0.5%, 1.0% and 3.0% and named as V0.1-TiO_2, V0.3-TiO_2, V0.5-TiO_2, V1.0-TiO_2 and V3.0-TiO_2, respectively. In addition, an undoped TiO_2 was also prepared by the same procedure for comparison. The reaction in the solution combustion could be given as below:

$$3TiO(NO_3)_2+2.5CO(NH_2)_2\rightarrow 3TiO_2+2.5CO_2+5.5N_2+14H_2O+3.75O_2 \quad (1)$$

2.2 Catalyst characterization

The phase of the powders was analyzed by the X-ray diffractometer (Netherlands, X'Pert PRO) with a Cu Kα radiation (λ=1.540 6 Å) at 40 kV tube voltage and 40 mA tube current in a 2θ ranging from 10° to 90°. Field emission scanning electron microscope (FEI, Sirion 200) was used to investigate the microstructures of the obtained powders. The Raman spectra were recorded on a RENISHAW Raman spectrometer equipped with an optical microscope at room temperature with an excitation of 632.8 nm laser light from an Ar+ ion laser. The chemical states of species were measured by a VG Multilab 2000 X-ray photoelectron spectroscope (XPS). The ultraviolet-visible diffuse reflectance spectra (UV-Vis DRS) of the samples were measured by a spectrophotometer (Shimadzu UV-2550). The obtained diffuse reflectance spectra were converted to absorption spectra on the basis of the Kubelka-Munk theory.

2.3 Photocatalytic experiments

The photocatalytic activities of TiO_2 powders were evaluated by the decomposition of methyl orange (MO) in water. The photocatalytic degradation was performed in a glass beaker in which 0.2 g TiO_2 powders were suspended in 100 mL MO solution (10 mg•L^{-1}). A high-voltage mercury lamp (500 W) with a maximum irradiation peak at 417 nm was used as a light source. A light filter was used to filter UV light whose wavelength is shorter than 400 nm. Prior to irradiation, the suspension was magnetically stirred for 30 min in dark to establish adsorption/degradation equilibrium for MO. The distance between the liquid surface and the light source was fixed at 25 cm. After irradiation for 10 h, 5 mL suspension was taken from the reaction cell and separated by centrifugation (10 000 rpm, 15 min). The absorption spectrum of the centrifuged solution was measured on a UV-Vis spectrophotometer (Shimadzu UV-2550). The concentration of MO was determined by monitoring the change in the absorbance at 550 nm.

3 Results and discussion

Fig.1 shows the XRD patterns of undoped and V-doped TiO_2 powders. All the samples exhibit TiO_2 diffraction peaks containing anatase and rutile and no characteristic peaks of vanadium oxides are observed. As presented in Fig.1(b), the peak position of rutile (110) plane of the V-doped TiO_2 powders shifts towards higher diffraction angles gradually with the V doping concentration increasing. These reveal that V ions have entered into TiO_2 crystal lattice to form a homologous solid solution. The shift of diffraction peaks is attributed to the substitution of V^{5+} for Ti^{4+}. The ionic radius of V^{5+} (0.68 nm) is smaller than that of Ti^{4+} (0.74 nm). As V^{5+} fills into Ti-site, the distortion of the

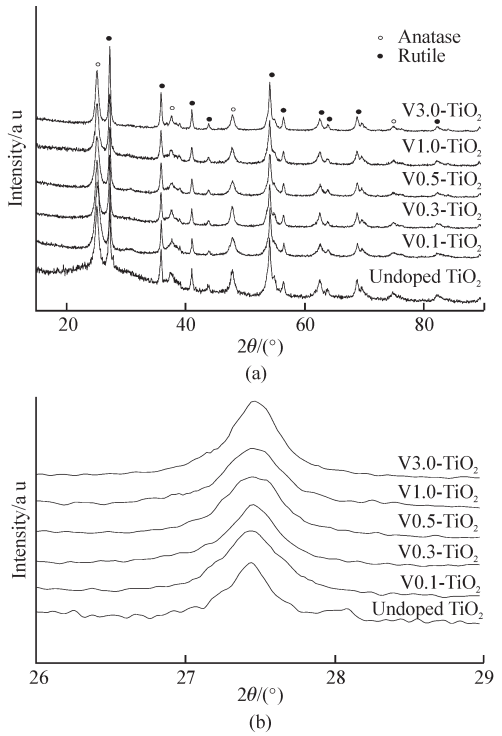

Fig.1 (a) XRD patterns of undoped and V-doped TiO_2 powders; (b) Magnification of XRD patterns in the 2θ ranges from 26° to 29°

crystal lattices induces the lattice constant to decrease, and then the diffraction peaks shift to higher diffraction angles.

The average crystalline sizes of anatase and rutile in the samples are calculated by the following Debye-Scherrer formula based on the anatase (101) and rutile (110) diffraction peaks:

$$D = \frac{K\lambda}{\beta \cos\theta} \tag{2}$$

where D is the crystallite size in angstroms, K is a constant which is taken as 0.89 here, λ is the radiation wavelength (0.154 05 nm for Cu Kα), β is the corrected band broadening (full width at half-maximum (FWHM)) after subtraction of equipment broadening and θ is the diffraction peak angle. The calculated values are listed in Table 1. The crystalline sizes of anatase and rutile increase with V doping concentration, which is similar to the reported results by Gu and Wu[15, 17].

The phase contents of anatase and rutile in the samples can be estimated from the respective XRD peak intensities using the following Eq. 3[18].

$$f_R = \frac{I_R}{0.884 I_A + I_R} \tag{3}$$

where f_R is the fraction of rutile in the powder, and I_A and I_R are the X-ray intensities of the anatase (101) and rutile (110) diffraction peaks, respectively. The contents of anatase and rutile in the samples are also shown in Table 1. As presented in Table 1, the content of rutile increases gradually with increasing V doping concentration while that of anatase decreases. This can be explained as following. Rutile is more thermodynamically stable than anatase. When Ti site is substituted by V ions, the lattice distortion decreases the thermal stability of anatase, promoting the phase transition from anatase to rutile[19]. In addition, the ionic radius of V^{5+} is slightly smaller than that of Ti^{4+}. As V^{5+} fills into Ti-site, the shrinkage of V-doped TiO_2 crystal lattices induces the formation of more compactly packed rutile (ρ_{rutile}=4.26 g/cm^3, $\rho_{anatase}$=3.84 g/cm^3) [20].

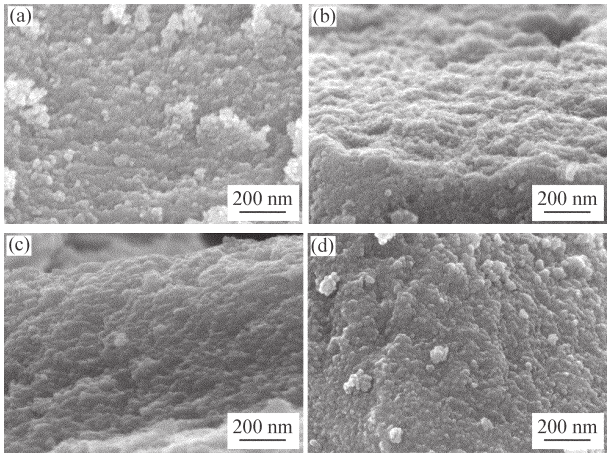

Fig.2 SEM images of undoped and V-doped TiO_2 powders: (a) undoped TiO_2; (b) V0.3-TiO_2; (c) V1.0-TiO_2; (d) V3.0-TiO_2

Fig.2 shows the SEM images of undoped and V-doped TiO_2 powders. It is found that all the samples exhibit agglomeration of fine primary particles which

Table 1 Physicochemical properties of undoped and V-doped TiO_2 samples

Sample	V Content/at%	Crystalline size of anatase[a]/nm	Crystalline size of rutile[a]/nm	Contents of anatase[b]/%	Contents of rutile[b] f_R/%
Undoped TiO_2	0.0	11.4	20.4	45.5	54.5
V0.1-TiO_2	0.1	12.2	24.0	44.3	55.7
V0.3-TiO_2	0.3	12.9	25.2	42.6	57.4
V0.5-TiO_2	0.5	14.3	26.6	41.4	58.6
V1.0-TiO_2	1.0	15.2	28.1	40.8	59.2
V3.0-TiO_2	3.0	17.4	31.3	38.1	61.9

[a] Calculated by Eq. 2; [b] Calculated by Eq. 3

are rather small in size (<50 nm) and spherical in shape. The morphology of the particles exhibits no obvious changes with the V doping concentration increasing.

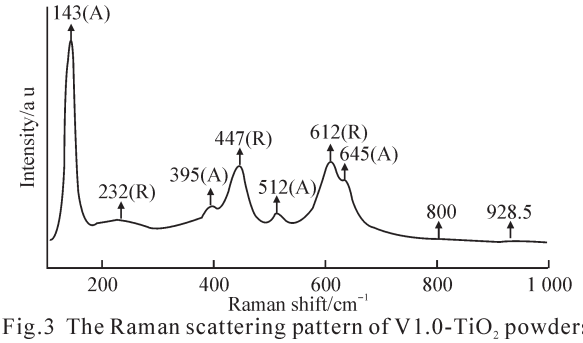

Fig.3 The Raman scattering pattern of V1.0-TiO_2 powders

Fig.3 shows the Raman pattern of V1.0-TiO_2 powders. The observed spectrum can be ascribed to the mixture of anatase (bands at 645, 512, 395 and 143 cm^{-1}) and rutile (bands at 612, 447 and 232 cm^{-1}), which is in agreement with the XRD result. Two unclear peaks at 800 and 928.5 cm^{-1} appeared on the Raman spectrum of V1.0-TiO_2 may indicate TiO_2 structural deformation after V doping[14]. The vibration peaks related to the V-O compounds are not observed, indicating no individual V-O phase in the V1.0-TiO_2 powders. Combined with the XRD analysis, it can be considered that V ions have been doped in the TiO_2 lattice but not in the form of VOx isolated phase. The result was in accordance with the literature[9].

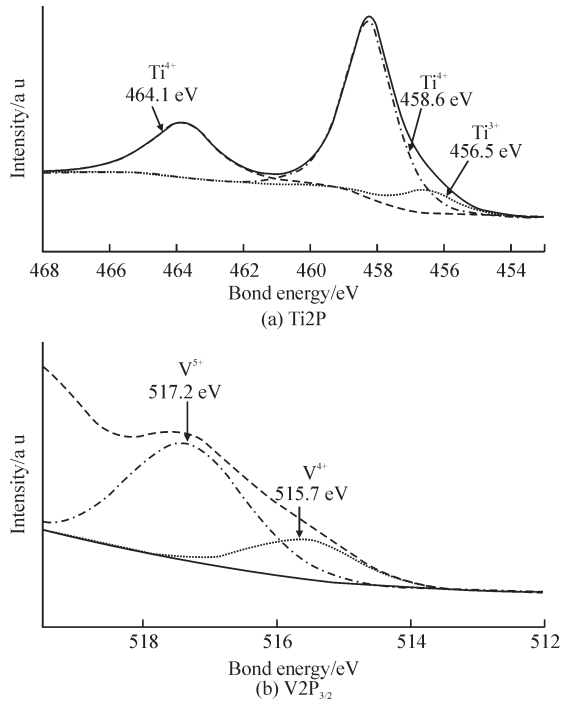

Fig.4 The Ti2p and V3p high-resolved XPS spectra of V1.0-TiO_2 powders

Fig.4(a) shows the XPS spectrum for Ti2p of V1.0-TiO_2 powders. The Ti2p peak splits into $Ti2p_{3/2}$ (458.4 eV) and $Ti2p_{1/2}$ (464.1 eV) due to self-orbital coupling effect. The $Ti2p_{3/2}$ peak is wider and more unsymmetrical than that of pure TiO_2, indicating that the V ion incorporates into the TiO_2 lattice and results in Ti_2O_3 formation accompanied by oxygen defects[14]. The $V2p_{3/2}$ XPS spectrum of that V1.0-TiO_2 powders is shown in Fig.4(b), which displays that V ions in the V-doped TiO_2 powders consist of two chemical states. They are V^{5+} at 517.2 eV and V^{4+} at 515.7 eV [14]. The $V2p_{1/2}$ cannot be observed because of the influence of the O1s satellite peak. The presence of V^{4+} in the mixture catalysts may be due to the reduction of V^{5+} by Ti^{3+} generated during the calcination of the catalysts[5].

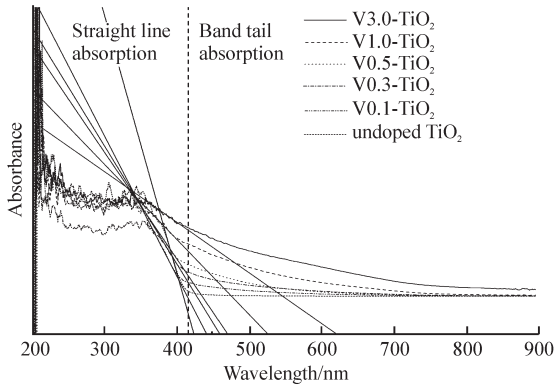

Fig. 5 UV-Vis absorption spectra of undoped and V-doped TiO_2 powders

Fig.5 shows the UV-Vis absorption spectra of undoped and V-doped TiO_2 samples. The absorption edge of undoped TiO_2 emerges at 425 nm. This value is slightly higher than the reported value of TiO_2, which may be attributed to the carbon inclusion into the TiO_2 giving $TiO_{2-2x}C_x[\ ]_x$ during the combustion synthesis process[21]. The band gaps (E_g) of all samples are estimated from the following equation[22]:

$$\alpha(h\nu) = A(h\nu - E_g)^{m/2} \quad (4)$$

where α is the absorption coefficient, $h\nu$ is the photon energy, and m =1 for a direct transition between bands. The values are listed in Table 2. Compared with the spectrum of pure TiO_2, the red shift is clearly observed in series of V-doped TiO_2 catalysts. The extent of red shift depends on the amount of V ions implanted. The higher the V dopes, the greater the red shift is. Such a shift allows the V-doped TiO_2 catalysts to use visible light irradiation more effectively. When the amount of V doping reaches 3.0 at%, the absorption edge of the powders is extended to 625 nm with a band gap of 1.87 eV. It has been reported that the red-shift of absorption edge was attributed to the charge-transfer transition between the d electrons of the

dopant and the conduction band (or valence band) of TiO_2[8]. In the case of V-doped TiO_2 powders, the red shift of absorption edge should be due to the electron transition from the VB (O 2p) to the t_{2g} level of V 3d orbit because V 3d orbit is located at the bottom of the conduction band of TiO_2.

Table 2 Physicochemical properties of undoped and V-doped TiO_2 samples

Sample	V content /%	Absorption edge/nm	Band gap[c] /eV
Undoped TiO_2	0.0	425	2.74
V0.1-TiO_2	0.1	443	2.63
V0.3-TiO_2	0.3	460	2.54
V0.5-TiO_2	0.5	472	2.47
V1.0-TiO_2	1.0	528	2.21
V3.0-TiO_2	3.0	625	1.87

[c] Calculated by Eq.(4)

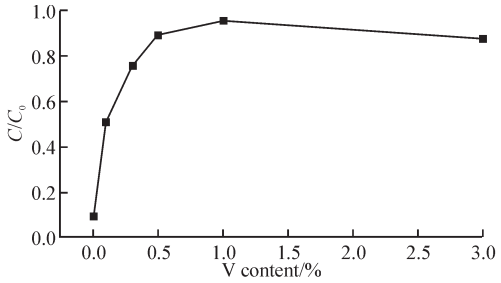

Fig.6 Photocatalytic degradation of MO solution (10 mg • L^{-1}) under visible light for 10 h over undoped and V-doped TiO_2 powders

Fig.6 shows the photocatalytic degradation of MO solution (10 mg•L^{-1}) under visible light for 10 h over undoped and V-doped TiO_2 powders. The photocatalytic activity of samples was evaluated by measuring the concentration (C/C_0) of MO, in which C_0 and C represent the initial equilibrium concentration and reaction concentration of MO, respectively. As can be seen from Fig.6, limited degradation of MO is detectable for undoped TiO_2 sample under visible light radiation. The photocatalytic activity of the samples increases sharply with V doping concentration increasing at the beginning and then decreases slightly, with the optimum degradation rate of 95.8% at 1.0 at% V doping concentration. This can be explained as following. An optimum V doping concentration for V-TiO_2 decreases the particle size, and thus promotes adsorption of organic compounds and photons in unit time and shortens the transition time for electron to the particle surface. In addition, an optimum V doping widens the light absorption range to the visible light region, which results in more photogenerated electron-hole pairs participating in the degradation of MO under visible light radiation. Furthermore, an appropriate amount of V doping makes the surface barrier higher and the space charge region narrower, the electron-hole pairs within the region are efficiently separated by the large electric field before recombination[11]. However, when the V doping concentration is high, the excessive V ions will cover the surface of the composite powders to hinder the absorption of light and act as electron-hole traps that promote the recombination of the photo-induced electron-hole pairs[23, 24].

4 Conclusions

Nanocrystalline V-doped TiO_2 catalysts have been fabricated by the one-step solution combustion method using nitrate as an oxidizer and urea as a fuel. V ions are successfully incorporated into the TiO_2 crystal lattice in the form of V^{5+} ions. V doping favors the primary particle size growth as well as the increase of rutile content in the products. Due to the excitation of electrons from the valence band of O 2p to the 3d orbit of V, V doping widens the light absorption range, with the absorption threshold wavelength shifting from 425 to about 625 nm. The degradation percentage of MO after 10 h on V1.0-TiO_2 powders is about 95.8%, indicating a good photocatalytic activity of the obtained V-doped TiO_2 powders.

Acknowledgments

The authors are thankful to the help from Analytical and Testing Center in Huazhong University of Science & Technology.

References

[1] H G Yu, H Irie, Y Shimodaira, *et al.* An Efficient Visible Light Sensitive Fe(III)-Grafted TiO_2 Photocatalyst[J]. *J. Phys. Chem. C*, 2010, 114(39): 16 481-16 487

[2] G D Yang, Z Jiang, H H Shi, *et al.* Preparation of Highly Visible Light Active N-doped TiO_2 Photocatalyst[J]. *J. Mater. Chem.*, 2010, 20, 5 301-5 309

[3] T D Bui, A Kimura, S Ikeda, *et al.* Determination of Oxygen Sources for Oxidation of Benzene on TiO_2 Photocatalysts in Aqueous Solutions Containing Molecular Oxygen[J]. *J. Am. Chem. Soc.*, 2010, 132(24): 8 453-8 458

[4] G Liu, C H Sun, X X Yan, *et al.* Iodine Doped Anatase TiO_2 Photocatalyst with Ultra-long Visible Light Response: Correlation Between Geometric/electronic Structures and Mechanisms[J]. *J. Mater. Chem.*, 2009, 19: 2 822-2 829

[5] S Klosek, D Raftery. Visible Light Driven V-Doped TiO_2 Photocatalyst and its Photooxidation of Ethanol[J]. *J. Phys. Chem. B*, 2001, 105: 2 815-2 819

[6] S In, A Orlov, R Berg, *et al.* Effective Visible Light-Activated B-Doped and B,N-Codoped TiO_2 Photocatalysts[J]. *J. Am. Chem. Soc*., 2007, 129: 13 790-13 791

[7] X J Quan, Q H Zhao, H Q Tan, *et al.* Comparative Study of Lanthanide Oxide Doped Titanium Dioxide Photocatalysts Prepared by Coprecipitation and Sol-gel Process[J]. *J. Mater. Chem Phys*., 2009, 114: 90-98

[8] W Choi, A Termin, M R Hoffmann. The Role of Metal Ion Dopants in Quantum-sized TiO_2: Correlation Between Photoreactivity and Charge Carrier Recombination Dynamics[J]. *J. Phys. Chem.*, 1994, 98: 13 669-13 679

[9] X X Yang, C Cao, K Hohn, *et al.* Highly Visble-light Active C- and V-doped TiO_2 for Degradation of Acetaldehyde[J]. *J. Catal*., 2007, 252: 296-302

[10] S T Martin, C L Morrison, M R Hoffmann. Photochemical Mechanism of Size-quantiezed Vanadium-doped TiO_2 Particles[J]. *J. Phys. Chem.*, 1994, 98: 13 695-13 704

[11] Z M Tian, S L Yuan, S Y Yin, *et al.* Synthesis and Magnetic Properties of Vanadium Doped Anatase TiO_2 Nanoparticles[J]. *J. Magn. Magn. Mater*., 2008, 320: L5-9

[12] M Anpo, Y Ichihashi, M Takeuchi, *et al.* Design of Unique Titanium Oxide Photocatalysts by an Advanced Metal Ion-implantation Method and Photocatalytic Reactions Under Visible Light Irradiation[J]. *Rse. Chem. Intermed.*, 1998, 24: 143-149

[13] W F Zhou, Q J Liu, Z Q Zhu, *et al.* Preparation and Properties of Vanadium-doped TiO_2 Photocatalysts[J]. *J. Phys. D: Appl. Phys.*, 2010, 43: 035 301-035 306

[14] B S Liu, X L Wang, G F Cai, *et al.* Low Temperature Fabrication of V-doped TiO_2 Nanoparticles, Structure and Photocatalytic Studies[J]. *J. Hazard. Mater*., 2009, 169: 1 112-1 118

[15] J C S Wu, C Chen. A Visible-light Response Vanadium-doped Titania Nanocatalyst by Sol-gel method[J]. *J. Photochem. Photobiol. A*, 2004, 163: 509-515

[16] H Yamashita, M Anpo. Application of an Ion Beam Technique for the Design of Visible Light-sensitive, Highly Efficient and Highly Selective Photocatalysts: Ion-implantation and Ionized Cluster Beam Methods[J]. *Catal. Surv. Asia*, 2004, 8: 35-45

[17] D E Gu, B C Yang, Y D Hu. A Novel Method for Preparing V-doped Titanium Dioxide Thin Film Photocatalysts with High Photocatalytic Activity Under Visible Light Irradiation[J]. *Catal. Lett*., 2007, 118: 254-259

[18] H Zhang, J F Banfield. Understanding Polymorphic Phase Transformation Behavior during Growth of Nanocrystalline Aggregates: Insights From TiO_2[J]. *J. Phys. Chem. B*, 2000, 104: 3 481-3 487

[19] B Z Tiana, C Z Li, F Gua, *et al*. Flame Sprayed V-doped TiO_2 Nanoparticles with Enhanced Photocatalytic Activity under Visible Light Irradiation[J]. *Chem. Eng. J*., 2009, 151: 220-227

[20] Z M Wang, G X Yang, P Biswas, *et al.* Processing of Iron-doped Titania Powders in Flame Aerosol Reactors[J]. *Powder Technol*., 2001, 114: 197-204

[21] K Nagaveni, M S Hegde, N Ravishankar, *et al.* Synthesis and Structure of Nanocrystalline TiO_2 with Lower Band Gap Showing High Photocatalytic Activity[J]. *Langmuir*, 2004, 20: 2 900-2 907

[22] E Sanchez, T Lopez. Effect of the Preparation Method on the Band Gap of Titania and Platinum-titania Sol-gel Materials[J]. *Mater. Lett*., 1995, 25, 271-275

[23] Q Luo, X W Li, Q Z Cai, *et al.* Preparation of Narrow Band Gap V_2O_5/TiO_2 Composite Films by Micro-arc Oxidation[J]. *Int. J. Miner. Metall. Mater.*, 2012, 19: 1 045-1 051

[24] X Yang, F Y Ma, K X Li, *et al.* Mixed Phase Titania Nanocomposite Co-doped with Metallic Silver and Vanadium Oxide: New Efficient Photocatalyst for Dye Degradation[J]. *J. Hazard. Mater*., 2010, 175: 429-38